An Overview of Array Signal Processing and Beam Forming Techniques

Vaibhav
S.N.University
Rachi, India

Shiv Sunder Lokesh
ECE Department
Gyan Vihar University
Jaipur, India

Abinet Tesfaye
Electrical Engineering
MeU,Africa
Illu Babora, Africa

Tasew Ababe
Electrical Engineering
MeU,Africa
Illu Babora, Africa

Abstract: For use as hydrophones, projectors and underwater microphones, there is always a need for calibrated sensors. Overview of multi path and effect of reflection on acoustic sound signals due to various objects is required prior to finding applications for different materials as sonar domes, etc. There is also a need to overview multi sensor array processing for many applications like finding direction of arrival and beam forming. Real time data acquisition is also a must for such applications.

Keywords: Array signal processing; Uniform linear array; Beam Forming; Delay and Sum Beam Former; Spatial FFT.

1. INTRODUCTION

Array signal processing is a part of signal processing that uses sensors that are organized in patterns, or arrays, to detect signals and to determine information about them as shown in Fig.1. One of the applications of array signal processing involves detecting acoustical signals. The sensor in this overview is Hydrophones.
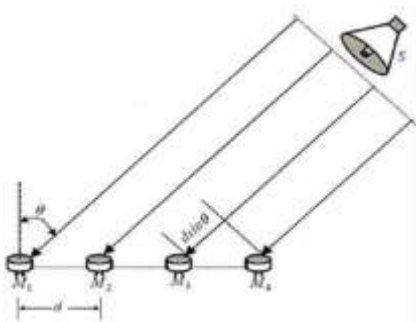

Figure 1: The uniform linear array

2. NEED

The goal of this overview is to develop an array which can listen from a specific direction, while attenuating signals not from the direction of interest. A six element uniform linear array can be created in order to determine the direction of the source of specific frequency signals. Because the uniform linear array is one dimensional, there is a surface of ambiguity on which it is unable to determine information about signals. For example, it suffers from "front-back ambiguity", meaning that signals incident from" mirror location" at equal angles on the front and back sides of the array undistinguishable. Without a second dimension, the uniform linear array is also unable to determine how far away a signal's source is or how high above or below the array's level the source is.

3. UNIFORM LINEAR ARRAY (ULA)

When constructing any array, the design specification should be determined by the properties of the signals that the array will detect. All acoustic waves travel at the speed 1500 m/s in underwater channel [6-8]. The physical relationship describing acoustic waves is similar to that of light $\lambda f = c$. The frequencies of signals that an array detects are important because they determine constraints on the spacing of the sensors. The array's sensors sample incident signal in space and, just as aliasing occur in analog to digital conversion when the sampling rate does not meet the Nyquist criterion, aliasing can also happen in space if the sensors are not sufficiently close together[3]. A useful property of the uniform linear array is that the delay from one sensor to the next is uniform across the array because of their equidistant spacing. Trigonometry reveals that the additional distance the incident signal travels between sensors is $dSin(\theta)$/Thus, the time delay between consecutive sensors is give

$$\zeta = dSin(\theta)/c \qquad (1)$$

Say the highest narrowband frequency we are interested is f_{max}. To avoid spatial aliasing, we would like to limit phase difference between spatially sampled signals to π or less because phase difference above π cause incorrect time delays to be seen between received signals. Thus, we give the following condition:

$$2\pi f_{max} \zeta \leq \pi \qquad (2)$$

Substituting for ζ from equation (1) into (2)

$$2\pi f_{max} dSin(\theta)/c \leq \pi \qquad (3)$$

$$d \leq c/2f_{max} Sin(\theta) \qquad (4)$$

The maximum delay according to equation 1 occurs for θ =90°, so we obtain fundamentally important condition from equation (4)

$$d \le c/2f_{max} \qquad (5)$$

For 40 KHz frequency spacing should be less than 1.87 cm according to equation (5). The direction perpendicular to the length of the array is taken as broadside of the array. All angles to the right or clockwise from the broadside are considered positive by convention up to +90°. All angles to the left or counter clockwise from the broadside are considered negative up to -90°.
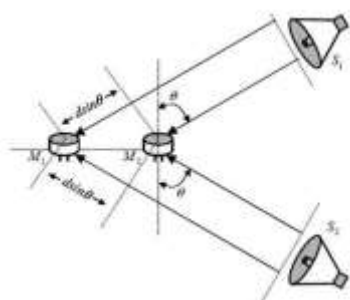
3.1 Ambiguity of the ULA

Figure 2 The ULA is unable to distinguish signals from its front or back side, or signals above or below it.

The limitation of the uniform linear array as shown in figure 2 create problem for locating acoustic source with much accuracy [4]. The array's design is highly extensible, however, and it is an important building block for more

4. BEAM FORMING

Beam forming is the process of trying to concentrate the array to sounds coming from only one particular direction. Spatially, this would look like a large double shaped lobby aimed in the direction of interest [5]. Making a beam former is crucial to meet one of the goals of the study which is to listen to sound in one direction and The best way to not listen noisy directions is to just steer all your energy towards listening in one direction. This is an important concept because it is not just used for array signal processing; it is also used in many sonar systems as well [1].

4.1 Delay and Sum Beam Former

It is good first step to implement delay and sum beam former, because it is the simplest example. The delay and sum beam former is based on the idea that if a uniform linear array is being used, then the output of each sensor will be the same, except that each one will be delayed by a different amount. So, if the output of each sensor is delayed appropriately then we add all the outputs together the signal that was For k= f n, and zero otherwise. Here normalized DFT is used.

Now the N spectra from each of the array's sensors according to equation (10) is calculated, to find how certain frequencies (of interest f_o from different angles with respect to the array's broadside) are distributed [7]. This DFT is performed by taking frequency component from each received signal that corresponds to f_o and concatenating them into an array. Then array is zero padded to make a length that is power of two in order to calculate the FFT. This FFT gives a spectrum that is digital sinc function centered at $f_o\zeta$. The value of the sinc represents the magnitude of the frequency f_o at an angle theta.

complex arrays such as cube, which uses multiple linear arrays or more exotic shapes such as a circle [1].

4.2 Spatial FFT Approach of Beam Forming

Let us consider the narrow band signals of the form

$$X(t)=\exp(j2\pi ft) \qquad (6)$$

Where, f is the frequency of the signal. If we have N sensors numbered from n=0,1……..N-1,Then the delayed version of x(t) that arrive at each hydrophone n are

$$Xn(t)=\exp(j2\pi f(t-n\zeta) \qquad (7)$$

Thus, the first sensor n=0 has zero delay, while the signal arrives at the second sensor n=1 one unit delay later then at the first, and so on for each sensor. Then, the signal is sampled at each hydrophones in the process of ADC, and let the sampled signal Xn (ζ) = Xn (mT), where m is the integer. This gives us the sampled sinusoids at each sensor

$$Xn(r) =\exp (j2\pi fr-n\zeta) \qquad (8)$$

Even though each sensor receives the same frequency signal, recall that delays X(t-nζ) in time correspond to modulation by exp(-jnζ) in frequency, so the spectra of the received signals at each sensor are not identical. The first discrete Fourier transform looks at the temporal frequency content at each sensor

$$Xn(k)=1/R^{1/2} \ \sum_{r=0}^{R=1} \exp\left(j2\pi f(r-n\zeta)\right) \exp\left(-\frac{j2\pi kr}{R}\right) \qquad (9)$$

$$Xn(k)=\exp(-j2\pi fn\zeta)/R^{1/2} \qquad (10)$$

Because of the shape of the lobes of the sinc, which look like beams at the various angles the process of using the array to look for signals in different directions is called beam forming. This technique is used frequently in array processing and enables detection of the direction of arrival of certain frequencies [2].
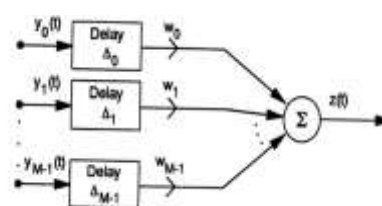

Figure 3 Sum and delay beam former

5. CONCLUSION

Basic theory of linear array is studied and constraints are derived that are useful for implementation of algorithms. The important condition for spacing between sensors of uniform linear array to avoid aliasing is derived in this overview.

6. REFERENCES

[1]   C.H. Cheng, "Signal Processing for Optical Communication," IEEE Signal Processing Magazine,

vol. 23, no. 1, pp. 88-96, 2006.

[2]   G. Keiser, "Optical Fiber Communication," McGraw-Hill International series, Third Edition, 2000.

[3]   C.D. Poole, J.M. Wiesenfeld, D.J. DiGiovanni, A.M. Vengsarkar, "Optical fiber-based dispersion compensation using higher order modes near cutoff," Journal of Lightwave Technology, vol. 12, no. 10, pp. 1746-1758, 1994.

[4]   N.M. litchinitser, D.B. Patterson, "Analysis of Fiber Bragg Gratings for Dispersion Compensation in Reflective and Transmissive Geometries," Journal of Lightwave Technology, vol. 15, no. 8, pp. 1303-1313, 1997.

[5]   D. Pastor, J. Capmany, D. Ortega, V. Tatay, and J. Marti, "Design of Apodized Linearly Chirped Fiber Gratings for Dispersion Compensation," Journal of Lightwave Technology, vol. 14, no. 11, pp. 2581–2588, 1996.

[6]   P.M. Watts, V. Mikhailov, S. Savory, P. Bayvel, M. Glick, M. Lobel, B. Christinsin, P. Krikpatrick, S. Shange, and R.I. Killey, "Performance of Single-Mode Fibers Links using Electronic Feed-Forward and Decision Feedback Equalizers," IEEE Photonics Technology Letter, vol. 17, no. 10, pp. 2206-2208,2005

[7]   S. Cao, J. Chen, J.N. Damask, C.R. Doerr, L. Guiziou, G. Harvey, Y. Hibino, H.Li, S. Suzuki, K.Y. Wu, and P. Xie, "Interleaver Technology: Comparisons and Applications Requirements," Journal of Lightwave Technology, vol. 22, no. 1, pp. 281-289, 2004.

[8]   S.K. Mitra, K. Hirano, "Digital All Pass Filters," IEEE transaction circuits and systems, vol. CAS 21, no. 9, pp. 688-700, 1974.

Power Factor Correction with Synchronous Condenser for Power Quality Improvement in Industrial Load

Moe Kay Thi Khaing
Mandalay Technological University
Mandalay, Myanmar

Abstract: As most of loads are of inductive type, the power system is in lagging power factor and as a result poor power quality is occurred. And it is demanded to make power factor correction to be better power quality of power system. Among power factor correction devices, synchronous condenser is studied in this paper to improve the industrial loads. There are ten numbers of induction motors in Tharpaung pulp plant and the net power factor of the factory power system is round about 0.85 lagging. By using 0.75 leading power factor of synchronous condenser, the system power factor is improved to 0.969 lagging. And it is studied to choose the appropriated synchronous condenser of power factor and rating for various system power factors. And if there are different operating times for each induction motors, which synchronous condenser should be run is studied in detail in the paper. It is shown that the use of synchronous condenser improves the system power factor and makes power quality better. In this study, MATLAB program is used for overall plant power factor calculation.

Keywords: inductive type, power factor, power quality, synchronous condenser, induction motor, lagging, leading

1. INTRODUCTION

Power quality is an important issue for distribution network companies. They must guarantee the electricity supply for the customers, while fulfilling certain quality requirements. The power quality problems with end-users in industrial load are power factor, under voltage, over voltage, voltage sag, voltage swell, voltage fluctuation, grounding, etc. Power factor is also a power quality issue in that low power factor can sometimes cause equipment to fail. In many instances, the cost of low power factor can be high; utilities penalize facilities that have low power factor because they find it difficult to meet the resulting demands for electrical energy. The study of power quality is about optimizing the performance of the power system at the lowest possible operating cost. Power factor is definitely an issue that qualifies on both counts [1].

Synchronous condensers are used principally in large power applications because of their high operating efficiency, reliability, controllable power factor, and relatively low sensitivity to voltage dips. They are constant-speed machines with applications in mills, refineries, power plants, to drive pumps, compressors, fans, pulverizers, and other large loads, and to assist in power factor correction. They are designed specifically for power factor control and have no external shafts, and are called synchronous condensers. It is floating on the system. It behaves as a variable capacitor when the field is over-excited, and as a variable inductor when the field is under-excited. In general, over excitation will cause the synchronous motor to operate at a leading power factor, while under exercitation will cause the motor to operate at a lagging power factor. Synchronous motor can also be used for power-factor correction in an industrial plant consisting of a large number of induction motors.

Power factor can be corrected with a capacitor. However, if a synchronous condenser is run with a leading power factor, it can perform useful work and correct power factor at the same time. In industrial applications where both synchronous condensers and induction motors are used, the synchronous condenser is usually operated at a leading power factor to compensate for the lagging power of the induction motors. An improved power also reduces the system voltage drop and the voltage drop at the terminals. Due to these advantages, synchronous condensers are used to improve power factor of the electrical system of a plant.

Therefore, appropriate rating of synchronous condenser is used with induction motors plant in this paper.

2. POWER FACTOR CORRECTION BY USING SYNCHRONOUS CONDENSER

Power factor correction usually means the practice of generating reactive power as close as possible to the load which requires it, rather than supplying it from a remote power station. The objective of power factor correction is to reduce the current flowing in the circuit connecting the load with the source of supply. When the power factor is high, the reactive component is a small percentage of the total and so a given change in the reactive component produces only a small change in the total. Accordingly, it is unnecessary to correct the power factor to exactly unity.

The power factor of a system can be improved by using a synchronous condenser and by varying its excitation. Increasing the strength of the magnets will increase the magnetic attraction and thereby the rotor magnets to have a closer alignment with the corresponding opposite poles of the rotating stator flux, the result is a smaller power angle. Assuming a constant shaft load, the steady-state value of $E_f \sin\delta$ must be constant. A step increase in E_f will cause a transient increase in $E_f \sin\delta$, and the rotor will accelerate. As the rotor changes its angular position, δ decreases until $E_f \sin\delta$ has the same steady-state value as before, at which time the rotor is again operating at synchronous speed. The change in angular position of the rotor magnets relative to the rotating flux of the stator occurs in a fraction of a second [2]. The effect of changes in field excitation on armature current, power angle, and power factor of a synchronous motor operating with a constant shaft load, from a constant voltage, constant frequency supply, is illustrated in Figure 1. For a constant shaft load,

$$E_{f1}\sin\delta_1 = E_{f2}\sin\delta_2 = E_{f3}\sin\delta_3 = E_f\sin\delta \qquad (1)$$
$$I_{a1}\cos\Phi_{i1} = I_{a2}\cos\Phi_2 = I_{a3}\cos\Phi_3 = I_a\cos\Phi_i \qquad (2)$$

This is shown in Figure 1, where the locus of the tip of the I_a phasor is a line perpendicular to the V_T phasor. Increasing the excitation from E_{f1} to E_{f3} in Figure 1 caused the angle of the current phasor to go from lagging to leading. The value of field excitation that results in unity power factor is called normal excitation. Excitation greater than normal is called overexcitation, and excitation less than normal is called

underexcitation. Furthermore, as indicated in Figure 1, when operating in the overexcited mode, $|E_f| > |V_T|$.

At minimum stator current, the motor is operating at unity power. If the field current value is held constant, Figure 2 will show the amount of leading kVA supplied to the line. At full load, the field excitation is sufficient to operate the motor at unity power factor for supplying no kVAR. The size of generator, transmission lines, transformers and distribution networks are based on the kVA demand, and the overall losses in these components are also determined by kVA. The electrical power in kilowatts consumed largely determines the fuel consume by the prime mover but in most systems the charges for electrical energy based on kVA demand and on kilowatts. It is usually economic, therefore, to operate a load of some power factor approaching unity, and when the power factor of a load is slow, the saving in power charges obtained by improving the power factor justifies the installation of special equipment for the purposes. The main advantage possessed by synchronous condenser is that the kVAR taken by it can be varied by adjusting the excitation. When such a machine is used to provide the power factor of a load, automatic control excitation can be used to keep the overall load power factor constant, within the capacity of the condenser by using a scheme such as has been described for a synchronous motor. In many cases, operation with fixed excitation is satisfactory and the condenser is then arranged to compensate for a fixed amount of lagging current taken by the load. For each load, there is definite limit beyond which it is not economical to raise the power factor as the increase in cost of equipment required is not compensated for by the reduction in power charges. Figure 3 shows the variation of percentage reduction in kVA demand for a fixed kilowatt load with the amount of power factor correction expressed as a percentage of the original kVA curves are shown for several values of power factor of the original load. The reduction in kVA demand can be increased until the maximum value, at unity power factor, is reached. The saving in power charges can be elevated for various size of condenser and the economic limit thus determined[3].
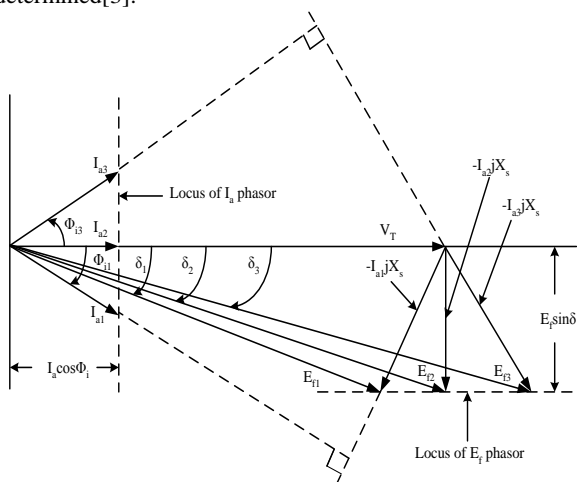

Figure. 1 Phasor diagram showing the effect of changes in field excitation on armature current, power angle, and power factor of a synchronous motor

The maximum amount of reduction in kVA which can be obtained increases of the original factor decreases, but it also involved as increase in the amount of condenser capacity required. The rate of change of reduction in kVA with increase in condenser rating decreases from the initial value to zero and it is therefore possible, by substituting appropriate

saving in cost due to reduced kVAR and capital cost required for condenser capacity to determine the most economic size of condenser for a given load condition.
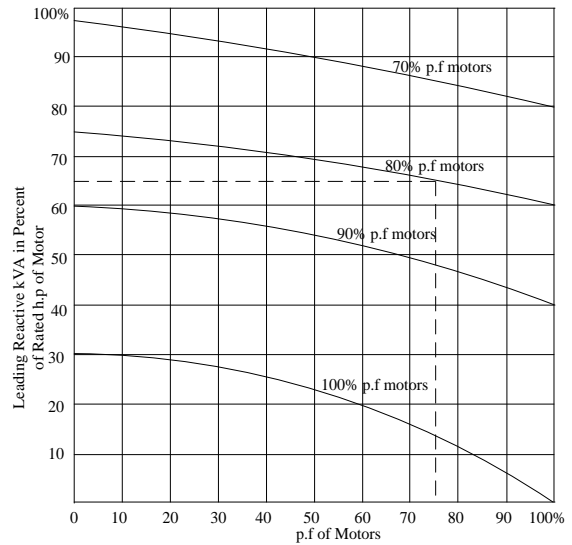

Figure. 2 Showing approximate leading kVA drawn by high speed synchronous motors operate at partial loads with full-load excitation maintained[4]
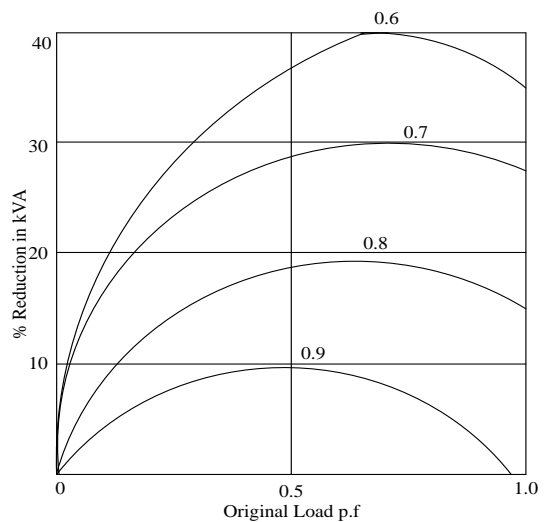

Figure. 3 Relationship between condenser rating reductions in kVA demand [3]

The real input power of the motor (kW) is:
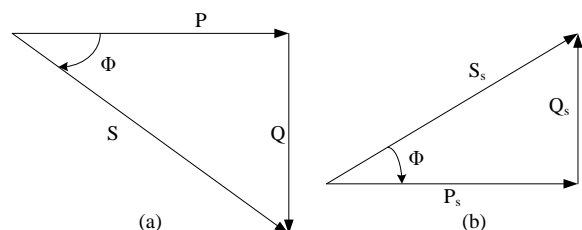
$$P = \frac{Output}{effeciency} \qquad (3)$$

Figure. 4 Phasor diagram of (a) induction motor and
(b) synchronous motor

The power factor (p.f) is:

$$p.f = cos\Phi = \frac{P}{S} \qquad (4)$$

The reactive power(kVAR) is:

$$Q = P\tan\Phi \qquad (5)$$

If all loads are induction motors in the system, total real power and reactive power of the system are:

$$P_T = \sum_{i=1}^{n} P_i \qquad (6)$$

$$Q_T = \sum_{i=1}^{n} Q_i \qquad (7)$$

If a synchronous condenser is added in the system of induction motors, total real power and reactive power are:

$$P_T = \sum_{i=1}^{n} P_i + P_s \qquad (8)$$

$$Q_T = \sum_{i=1}^{n} Q_i - Q_S \qquad (9)$$

Power factor of the system is:

$$p.f_T = cos(\tan^{-1}(\frac{Q_T}{P_T})) \qquad (10)$$

If Total reactive power of induction motors is greater than reactive power of synchronous condenser, power factor of the system is lagging. Otherwise, it is leading.

Where, S=apparent power(kVA)

P_S= real power of synchronous condenser

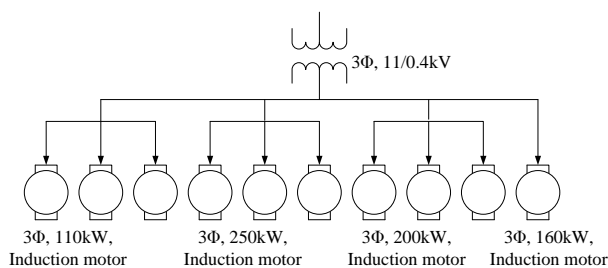Q_S=reactive power of synchronous condenser

3. SYSTEM OF CASE STUDY

Figure. 5 One line diagram of system

The designed paper plant consists of ten numbers of induction motors for paper making. There are three numbers of 110 kW induction motor used for first refiner, three numbers of 250 kW induction motor used for second refiner, three numbers of 200 kW induction motor used for third refiner and a 160 kW induction motor used for Hydrapulper. The desired plant is shown in Figure 5. These machines are operated with full load or light load. And then they are operated with all together or some of them. Therefore, various cases are considered in this study.

Table 1. Total installed ratings

Output (kW)	η (%)	p.f	No:	Total absorption P(kW)	Q(kVAR)
110	94	0.86	3	351.064	208.306

250	94.5	0.81	3	793.651	574.592
200	94.6	0.88	3	634.249	342.337
160	94.2	0.86	1	169.851	100.782
Total				1948.815	1226.017
p.f of the system			0.846		

4. COMPARISON RESULTS BY USING DIFFERENT RATINGS OF SYNCHRONOUS CONDENSER

There are different ratings of synchronous motors available in the market. The study is done based on the rating of 210kW, 480kW, 600kW, 800kW, 1400kW and 2400kW. Different rating of synchronous motor varies the overall plant power factor. The power factor of overall plant is limited within 0.95 lagging and unity. Various ratings of synchronous motor are considered at 0.75 leading, 0.8 leading, 0.85 leading, 0.9 leading, 0.95 leading and unity of power factor for 50%, 75%, 100% and 125% change of load.

Table 2. Results by using 210kW synchronous condenser

% of load	p.f of synchronous condenser					
	0.75 (lead:)	0.8 (lead:)	0.85 (lead:)	0.9 (lead:)	0.95 (lead:)	1
50	0.9447 (lag:)	0.9373 (lag:)	0.9297 (lag:)	0.9215 (lag:)	0.9118 (lag:)	0.8902 (lag:)
75	0.9191 (lag:)	0.9132 (lag:)	0.9073 (lag:)	0.901 (lag:)	0.8937 (lag:)	0.8778 (lag:)
100	0.9040 (lag:)	0.8989 (lag:)	0.8942 (lag:)	0.8892 (lag:)	0.8834 (lag:)	0.8709 (lag:)
125	0.8936 (lag:)	0.8897 (lag:)	0.8857 (lag:)	0.8815 (lag:)	0.8767 (lag:)	0.8664 (lag:)

Table 3. Results by using 480kW synchronous condenser

% of load	p.f of synchronous condenser					
	0.75 (lead:)	0.8 (lead:)	0.85 (lead:)	0.9 (lead:)	0.95 (lead:)	1
50	0.9941 (lag:)	0.9882 (lag:)	0.9806 (lag:)	0.9710 (lag:)	0.9579 (lag:)	0.9243 (lag:)
75	0.9729 (lag:)	0.9649 (lag:)	0.9563 (lag:)	0.9465 (lag:)	0.9344 (lag:)	0.9063 (lag:)
100	0.9537 (lag:)	0.9460 (lag:)	0.9379 (lag:)	0.9291 (lag:)	0.9186 (lag:)	0.8950 (lag:)
125	0.9387 (lag:)	0.9316 (lag:)	0.9244 (lag:)	0.9167 (lag:)	0.9074 (lag:)	0.8872 (lag:)

Table 4. Result by using 600kW synchronous motor

% of load	p.f of synchronous condenser					
	0.75 (lead:)	0.8 (lead:)	0.85 (lead:)	0.9 (lead:)	0.95 (lead:)	1
50	0.9995 (lag:)	0.9966 (lag:)	0.9910 (lag:)	0.9827 (lag:)	0.9701 (lag:)	0.9347 (lag:)
75	0.9859 (lag:)	0.9787 (lag:)	0.9703 (lag:)	0.9603 (lag:)	0.9474 (lag:)	0.9160 (lag:)
100	0.9687 (lag:)	0.9607 (lag:)	0.9522 (lag:)	0.9426 (lag:)	0.9307 (lag:)	0.9037 (lag:)
125	0.9537 (lag:)	0.9460 (lag:)	0.9379 (lag:)	0.9291 (lag:)	0.9186 (lag:)	0.8949 (lag:)

Table 5. Result by using 800kW synchronous condenser

% of load	p.f of synchronous condenser					
	0.75 (lead:)	0.8 (lead:)	0.85 (lead:)	0.9 (lead:)	0.95 (lead:)	1
50	0.9972 (lead:)	0.9999 (lead:)	0.9989 (lag:)	0.9940 (lag:)	0.9837 (lag:)	0.9480 (lag:)
75	0.9973 (lag:)	0.9927 (lag:)	0.9859 (lag:)	0.9768 (lag:)	0.9638 (lag:)	0.9292 (lag:)
100	0.9859 (lag:)	0.9787 (lag:)	0.9703 (lag:)	0.9603 (lag:)	0.9474 (lag:)	0.9160 (lag:)
125	0.9729 (lag:)	0.9649 (lag:)	0.9563 (lag:)	0.9465 (lag:)	0.9344 (lag:)	0.9063 (lag:)

Table 6. Result by using 1400kW synchronous condenser

% of load	p.f of synchronous condenser					
	0.75 (lead:)	0.8 (lead:)	0.85 (lead:)	0.9 (lead:)	0.95 (lead:)	1
50	0.9619 (lead:)	0.9797 (lead:)	0.9922 (lead:)	0.9990 (lead:)	0.9987 (lag:)	0.9704 (lag:)
75	0.9912 (lead:)	0.9978 (lead:)	0.9999 (lead:)	0.9978 (lag:)	0.9896 (lag:)	0.9547 (lag:)
100	0.9997 (lead:)	0.9995 (lag:)	0.9962 (lag:)	0.9894 (lag:)	0.9778 (lag:)	0.9419 (lag:)
125	0.9984 (lag:)	0.9944 (lag:)	0.9882 (lag:)	0.9793 (lag:)	0.9665 (lag:)	0.9315 (lag:)

Table 7. Results by using 2400kW synchronous condenser

% of load	p.f of synchronous condenser					
	0.75 (lead:)	0.8 (lead:)	0.85 (lead:)	0.9 (lead:)	0.95 (lead:)	1
50	0.9069 (lead:)	0.9381 (lead:)	0.9643 (lead:)	0.9847 (lead:)	0.9980 (lead:)	0.9852 (lag:)
75	0.9491 (lead:)	0.9706 (lead:)	0.9867 (lead:)	0.9969 (lead:)	0.9998 (lag:)	0.9748 (lag:)
100	0.9750 (lead:)	0.9885 (lead:)	0.9969 (lead:)	0.9999 (lead:)	0.9963 (lag:)	0.9649 (lag:)
125	0.9898 (lead:)	0.9971 (lead:)	0.9999 (lead:)	0.9982 (lag:)	0.9905 (lag:)	0.9559 (lag:)

The power factor using the ratings of 800kW, 1400kW and 2400kW are within limit, but they are large and more cost. The range of power factor by using 600kW synchronous motor can operate the plant load changing within restricted region. There are of four-load shedding at the plant. If it is required to shed the load, varying the power factor of the synchronous motor can be affective the plant operation.

Results for load shedding by using 600kW synchronous motor are shown in Table 9 Instead of 600kW synchronous motor,

Table 8. Results for percent load changing by using 600kW synchronous condenser

% change of load	p.f of synchronous condenser (lead:)
50	0.95~0.75
75	0.9~0.75
100	0.85~ 0.75
125	0.75

Table 9. Results for load shedding by using 600kW synchronous condenser

Induction motors in used		p.f of synchronous condenser (Lead:)
kW	No:	
110	3	0.99
110 250	3 3	0.989
110 250 200	3 3 3	0.835
110 250 200 160	3 3 3 1	0.75

Table 10. Results for load shedding by using three numbers of 200kW synchronous condensers

Induction motors in used		No: of synchronous condenser
kW	No:	
110	3	1
110 200	3 3	
200 160	3 1	
110 250	3 3	2
250 200	3 3	
110 250 200 160	3 3 3 1	

three numbers of 200kW synchronous motor can be used in the plant. And the results are shown in Table 10. In this table, only one 200kW synchronous motor can be used for running with three numbers of 110kW induction motors or three numbers of 110kW and three numbers of 200kW induction motors or three number of 200kW and a 160kW induction motors. Other load conditions are also shown in the table.

5. DISCUSSION

Loads used in domestics or industries are mostly inductive loads. Induction motor is that load. As inductive effect, power factor is lagging and it causes the system energy losses. Due to the effect, the load current is high, unload balancing is occurred and power quality is bad. From the point of view of economic, it also costs for the energy losses. For all cases, power factor improvement is needed for the system and compensators are essentially required.

In the study, a synchronous condenser or synchronous motor is used in parallel with induction motors as a compensator in the plant. As there are all type of induction motors, the plant overall power factor is also lagging. So synchronous motor with power factor leading is used to improve the plant power factor. Although unity power factor is the best one for the system, it is difficult to become nearly unity power factor of the system in practice but in theory. So there is limited range of plant power factor between unity and 0.95 lagging. For that why, the study is to drive the plant to be with limited power factor range.

To compensate the lagging power factor load to be unity one, the synchronous condenser must operate in leading power factor mode. Higher lagging power factor load needs higher leading power factor compensator. To be high power factor leading synchronous condenser needs larger excitation. So the study has not tried to be the plant power factor to be unity, but to be within the limit nearly 0.97 and 0.96.

In the study, there is only one synchronous condenser of 600kW in use to compensate the plant. And it also shows the data for the plant load changing. According to the results data, by varying the power factor of synchronous condenser, the plant power factor will be its limited range when it is needed to reduce or increase its load. As the limited value is within the range, six ratings of synchronous condenser power factor can drive the plant load in changed to be acceptable value.

6. CONCLUSION

In comparison with other compensators such as capacitor banks, reactors, synchronous condenser has some advantages in varying power factor. When load changing is encountered in the system, by easily varying the excitation system of synchronous condensers, the desired value has been in the system. Others compensators need to change add or reduce the components. But synchronous condenser is rotating machine, it can be needed some maintenance and it will cause some losses. As the operation of synchronous condenser can vary, it needs operator. So sometime fault operations may encounter in the system.

Instead of varying one synchronous condenser, a number of synchronous condensers being in used together should be studied in further study. The comparison should be made in the cost of capacitor banks and the cost of synchronous condensers, and the unit changes for using synchronous condensers. As the initial cost of synchronous condenser is large and as well its operating cost, it is needed to know about the synchronous machine, how to operate the machine, and how to control the machine. And as power factor adjustment is done by exciter, excitation systems of the machine are also important facts. As instead of 600kW synchronous condenser, three numbers of 200kW synchronous condenser can be used, further study should be done to find the merits using low rating of synchronous condenser in numbers.

7. ACKNOWLEDGMENTS

8. REFERENCES

[1] C. Sankaran, Power Quality, CRC Press LLC, Printed in the United States of America, 2002.

[2] +5V-Powered, Multichannel RS-232 Drivers/Receivers, May 2005, http://www.maxim.ic.com/packages..

[3] Data Sheet of Silicon Epitaxial Planner Type Diode, 1S1585_1S1588, February 2006, http://www.datasheetarchive.com.

[4] John Webb/Kevin Greshock, Industrial Control Electronic, May 2003.

[5] Leonard L. Grigsby, Electric Power Generation, Transmission and Distribution, Talor and Francis Group, CRC Press LLC, 2006.

[6] R. Sastry Vedam Mulukutla and S. Sarma, Power Quality VAR Compensation in Power Systems, Tallor and Francis Group, CRC Press LLC, 2009.

[7] Roger C.Dugan, Mark F. McGranaghan, Surya Santoso, H. Wayna Beaty, Electrical Power System Quality, Second edition, 2004 by Mc Graw-Hill.

[8] Hand Book of Power Quality, edited by Angelo Baggini, University of Bergamo, Italy, copyright by John Wiley and Sons Ltd, 2008.

Vulnerability of Flood Hazard in Selected

Ayeyarwady Delta Region, Myanmar

Khin Thandar Win
Department of Civil
Engineering
Mandalay Technological
University
Mandalay, Myanmar

Nilar Aye
Department of Civil
Engineering
Mandalay Technological
University
Mandalay, Myanmar

Kyaw Zaya Htun
Department of Remote Sensing
Mandalay Technological
University
Mandalay, Myanmar

Abstract: Flood disaster is a function of both natural hazard and vulnerable environs. It is needed to identify the flood hazard area for proper management and mitigation damage. River flood occurs because of heavy rainfall and geomorphology. In this study, Flood vulnerable areas for different return period flood are assessed by using Hydrologic Engineering Center's River Analysis System (HEC-RAS) model, GIS and Remote Sensing technique. Flood vulnerability analysis is carried out by overlaying the land use map and flood hazard map generated by the hydraulic model. GIS can be used to create interactive map overlays, which clearly illustrate which areas of a community are in danger of flooding. The main objective is to assess the flood vulnerable areas. Special attention of the concerned area on this disaster should be done to minimize loss from damage.

Keywords: flood hazard area; GIS and Remote Sensing; HEC-RAS; River flood; vulnerable.

1. INTRODUCTION

Myanmar's high vulnerability to natural disasters results from its unique geographic location. Ayeyarwady delta region is the worst flood affected region as it is located in low lying area. Due to this, it is necessary to do hazard assessment in order to know how much area would be the damage if a hazard occurs. An important prerequisite for developing management strategies for the mitigation of extreme flood events is to identify areas of potentially high risk to such events, thus accurate information on the extent of floods is essential for flood monitoring, and relief. Hydraulic modeling, especially HEC-RAS model is used to carry out the flood simulation to produce flood level at various locations along the river.

2. DESCRIPTION OF STUDY AREA

The study area is located between North latitude of 17°00' and 17°40' and East longitude of 95° 20' and 95° 50'. The drainage area of the study basin is about 2606.1km^2. The length of the river in the study area is 121.061km. The study area falls under the Ayeyarwady Regional Division.

3. DIGITAL ELEVATION MODEL

DEM is the digital elevation of the topographic surface. DEM must be a continuous surface that includes the bottom of the river channel and the floodplain to be modeled. DEM is also used to calculate the flooded depth by incorporating it into HEC-RAS flood modeling software. Because all cross-section data will be extracted from the DEM, only high-resolution DEM that accurately represent the ground surface should be considered for hydraulic modeling. Measurement units used are those relative to the DEM coordinate system.

4. LANDUSE CLASSIFICATION

To obtain the land use data of the study area, IRS satellite image of 2010 was classified in ENVI software. The following four types of land use classes were reclassified; agricultural land, forest, residential and water or herbaceous
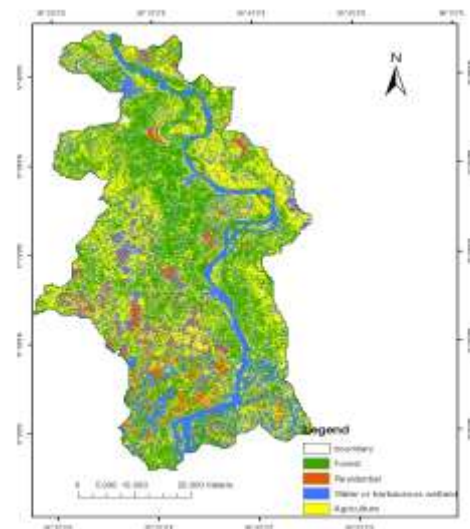
wetland (Figure1).

Figure1. Landuse map

5. METHODOLOGY

HEC-RAS model is chosen for flood inundation mapping and thereby to produce flood hazard maps correspond to 10, 20, 50 and 100 years return period flooding events [5]. The discharge data set for the inundation model was produced from the rainfall-runoff modeling. Flood hazard assessment is carried out using GIS and HEC-RAS [6]. Vulnerable areas are identified for 10, 20, 50 and 100 years return period flood. The general method adopted for flood hazard analysis are (1) Pre-processing of geometry data to generate HEC-RAS import file (2) Running of HEC-RAS to calculate water surface profiles (3) Post-processing of HEC-RAS results and floodplain mapping (4) flood hazard analysis and mapping and (5) Assess flood vulnerable areas.

5.1 Hydraulic Modeling

HEC-RAS is the hydraulic model which is used to calculate the water-surface profiles and energy grade lines in 1-D, steady-state, gradually-varied flow analysis. Knowing water surface elevation under various flow conditions, it is possible to evaluate flooding depth [1]. The data needed are geometry data and steady flow data. Geometry data are required for any of the analyses performed within HEC-RAS [1]. The basic geometric data consists of establishing the connectivity of the river system, cross-section data, reach length, energy loss coefficient.

5.2 Geospatial Hydraulic Modeling

HEC-GeoRAS is a set of ArcGIS tools specifically designed to process geospatial data. The extension allows users with limited GIS experience to create an HEC-RAS import file containing geometric data from existing digital elevation model (DEM). Results exported from HEC-RAS may be processed. The current version of HEC-GeoRAS creates import files containing reach, station identifiers, cross-sectional cutlines, and cross-sectional bank stations; downstream reach length for the left overbank, main channel, and right overbank and cross sectional roughness coefficients. Water surface profile data exported from HEC-RAS may be processed into GIS data sets [1]. Process flow diagram is shown in Figure 2.
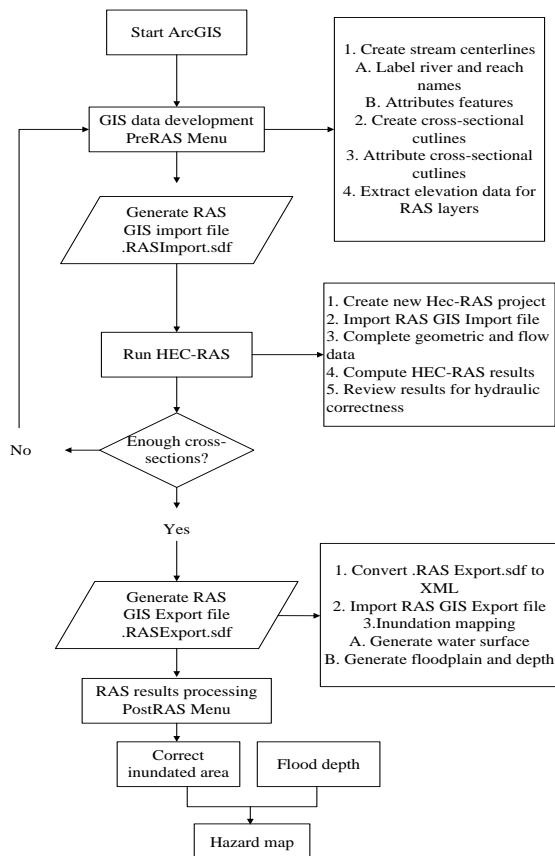
Figure 2. Process flow diagram of flood hazard mapping

5.2.1 Cross Section Data

Cross-sections are one of the key inputs to HEC-RAS. Cross-section cutlines are used to extract the elevation data from the terrain to create a ground profile across channel flow. The intersection of cutlines with other RAS layers such as centerline and flow path lines are used to compute HEC-RAS attributes such as bank stations (locations that separate main channel from the floodplain), downstream reach lengths (distance between cross-sections). Therefore, creating adequate number of cross-sections to produce a good representation of channel bed and floodplain is critical. Guidelines must be followed in creating cross-section cutlines: (1) they are digitized perpendicular to the direction of flow; (2) must span over the entire flood extent to be modeled; and (3) always digitized from left to right (looking downstream).
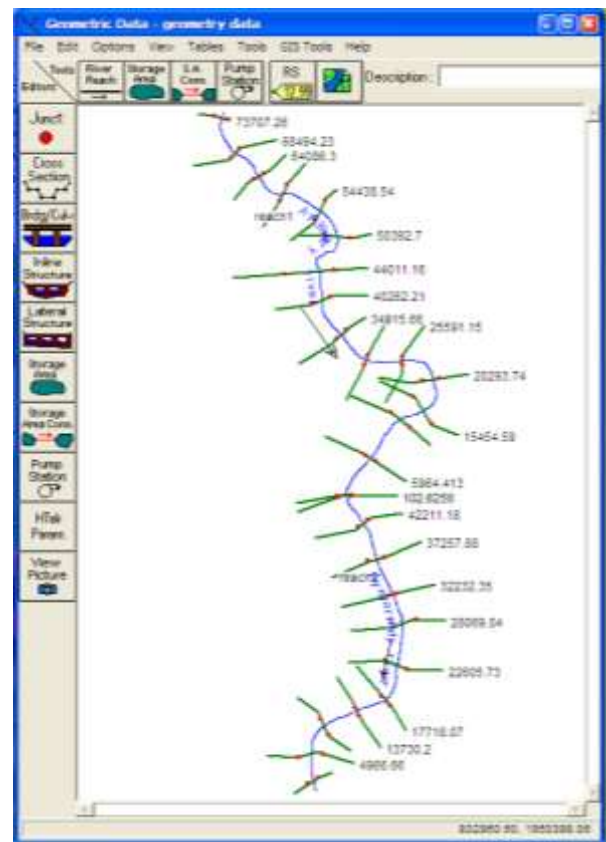

Figure 3. Schematic view of geometry of study river

5.2.2 Flow and Boundary Condition

The amount of flow through the system has to be entered along with certain boundary conditions before running the program to compute the desired results. Determining which boundary conditions are required depends on the conditions of the system and the type of model being run. In this study, steady flow analysis using a subcritical flow regime is used. Steady flow analysis consists of flow regime, boundary condition, and peak discharge information. Peak discharges are simulated by the hydrologic model [2][3].

6. RESULTS OF FLOOD HAZARD ANALYSIS

Flood hazard map shows area which could be flooded according to three probabilities (low, medium, high) complemented with flood extent and water depth or level [7].
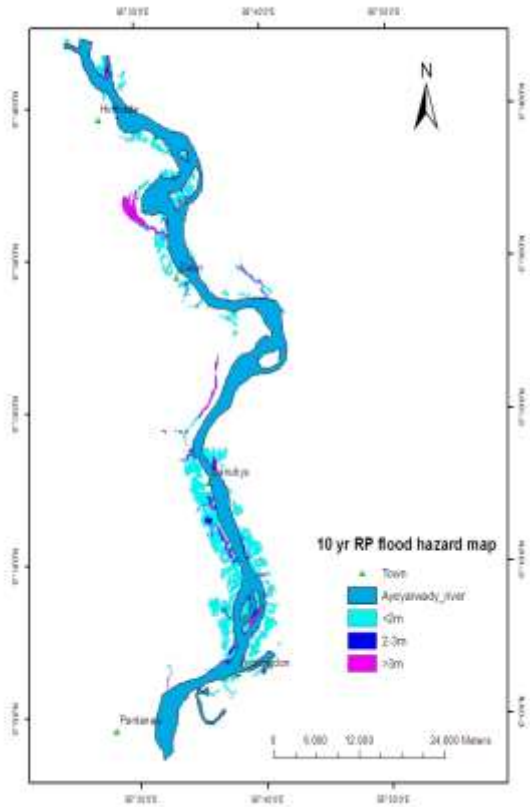

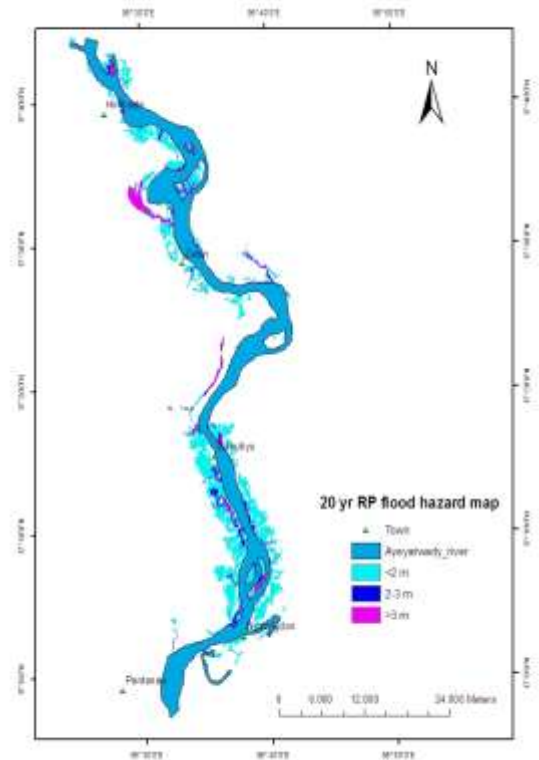Figure 4. Flood hazard map for 10 year return period flood

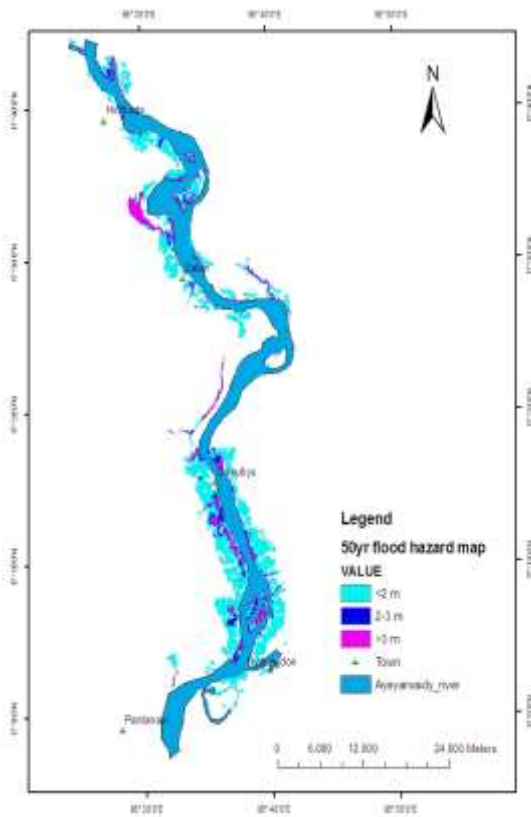Figure 5. Flood hazard map for 20 year return period flood

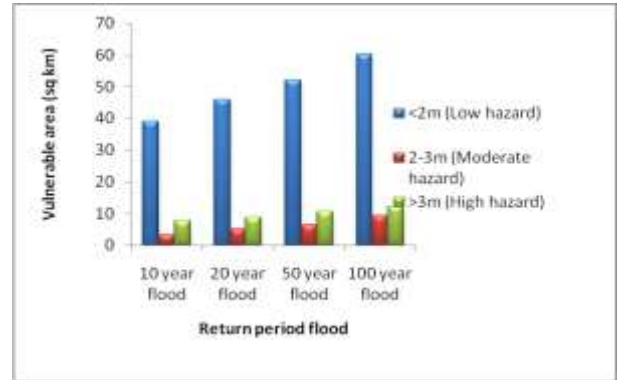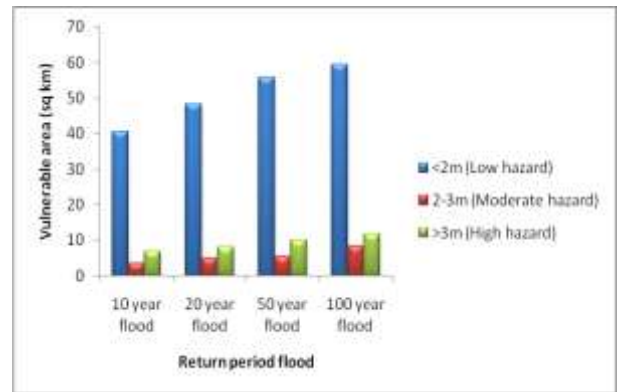Figure 6. Flood hazard map for 50 year return period flood

Figure 7. Flood hazard map for 100 year return period flood

Figure 8. Flood vulnerable area on agriculture

Figure 9. Flood vulnerable area on forest
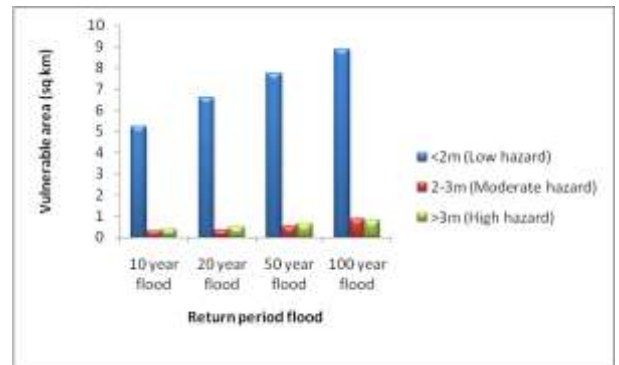
Figure 10. Flood vulnerable area on residential area
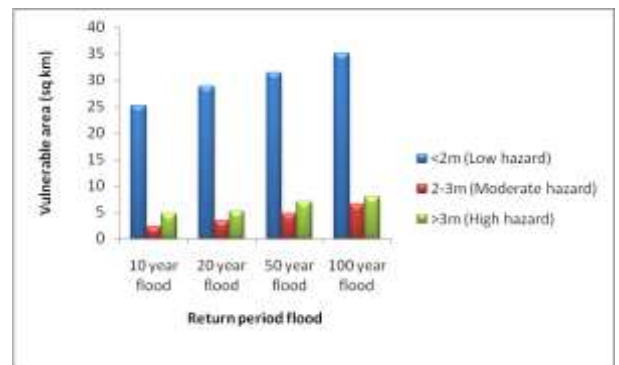
Figure 11. Flood vulnerable area on herbaceous wetland

Table 1. Vulnerable areas for 10 years and 20 years flooding

Landuse type	Flood depth	Total vulnerable area			
		10yr flood		20yr flood	
		km²	%	km²	%
Agriculture	<2m	38.9	27.9	45.9	27.6
	2-3m	3.3	2.4	5.07	3.1
	>3m	7.7	5.5	8.9	5.4
Forest	<2m	40.5	29.0	48.3	29.0
	2-3m	3.62	2.6	5	3.0
	>3m	7.05	5.1	8.14	4.9
Residential area	<2m	5.2	3.7	6.6	3.9
	2-3m	0.3	0.2	0.36	0.22
	>3m	0.4	0.3	0.49	0.3
Herbaceous wetland	<2m	25.2	18.0	28.8	17.4
	2-3m	2.4	1.7	3.4	2.0
	>3m	4.7	3.4	5.2	3.1
Total		139	100	166	100

Table 2. Vulnerable areas for 50 years and 100 years flooding

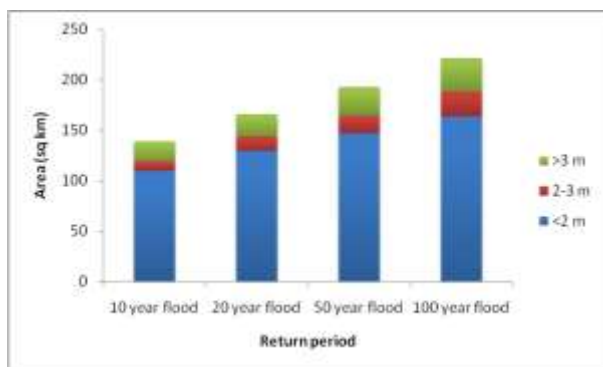| Landuse type	Flood depth	Total vulnerable area			
		50yr flood		100yr flood	
		km²	%	km²	%
Agriculture	<2m	51.9	26.9	60.2	27.2
	2-3m	6.3	3.3	9.3	4.2
	>3m	10.8	5.6	12.2	5.5
Forest	<2m	55.9	29.0	59.3	26.8
	2-3m	5.4	2.8	8.3	3.7
	>3m	10.2	5.3	11.8	5.3
Residential area	<2m	7.7	4.0	8.9	4.0
	2-3m	0.5	0.3	0.9	0.4
	>3m	0.6	0.3	0.8	0.4
Herbaceous wetland	<2m	31.4	16.3	35.0	15.8
	2-3m	4.7	2.4	6.6	2.9
	>3m	7.0	3.7	7.9	3.6
Total		192	100	221	100

Figure 12. Evaluation of total flood area according to flood hazard

7. CONCLUSION

According to the classification of flood hazard, flood depth less than 2 m has low hazard, flood depth between 2m and 3m has moderate hazard and flood depth greater than 3m has high hazard. About 14 % of the total flood areas in all flood events tend to have high hazard. The total areas under moderate hazard are 6.8 % on 10 year flood, 8.3 % on 20 year flood, 8.8 % on 50 year flood and 11.4 % on 100 year flood. Similarly, 78.9 %, 77.9 %, 76.2 % and 73.8 % of the total flood areas for 10 year, 20 year, 50 year and 100 year are under low hazard. Agriculture and forest are the most vulnerable to different return period flooding. Flood occurs in residential area every year with low hazard (flood depth of less than 2 meters).

8. ACKNOWLEDGMENTS

9. REFERENCES

[1] Hydrologic Engineering Center, "User manuals of river analysis system, HEC-RAS (version 3.1)", 2002.

[2] Hydrologic Engineering Center, "User manuals of hydrologic modeling system, HEC-HMS (version 3.5)", 2002.

[3] Hadi Tahmasbinejad, Mehdi Feyzolahpour, Mehdi Mumipour and Fatemeh Zakerhoseini, "Rainfall-runoff simulation and modeling of Karun river HEC-HMS model, Izeh district, Iran," Science Alert journal, Sept. 2012.

[4] Dilip Kumar, and Rajib Kumar Bhattacharjya, "Distributed Rainfall Runoff Modeling," International Journal of Earth Sciences and Engineering ISSN 0974-5904, Vol. 04, No 06 SPL, pp. 270-275, Oct. 2011.

[5] J.S.M. Fowze, H.K.Nandalal, D.P. Welideniya and S.M.J.S. Samarasinge, "Flood inundation modeling in the lower reach of the Kalu river, Sri Lanka,"

[6] Sina Alaghmand, "River modeling for flood risk map prediction: case study of Sungai Kayu Ara," M.Science. thesis, University Sains, Malaysia, July. 2009.

[7] Shantosh Karki, "GIS based flood hazard mapping and vulnerability assessment of people due to climate change: case study from Kankai watershed, East Nepal,' report, National Adaptation Programme of Action (NAPA), Nepal, Jan.2011.

Design of STT-RAM cell in 45nm hybrid CMOS/MTJ process

Karrar Hussain
CVR College of Engineering
Andhra Pradesh, India

Dr. C V Krishna Reddy
NNRES
Andhra Pradesh, India

Dr. K Lal Kishore
JNTU - Anantapur
Andhra Pradesh, India

Abstract: This paper evaluates the performance of Spin-Torque Transfer Random Access Memory (STT-RAM) basic memory cell configurations in 45nm hybrid CMOS/MTJ process. Switching speed and current drawn by the cells have been calculated and compared. Cell design has been done using cadence tools. The results obtained show good agreement with theoretical results.

Keywords: STT-RAM, Magnetic Tunnel Junction (MTJ), Perpendicular Magnetic Anisotropy (PMA), Hybrid CMOS/MTJ process.

1. INTRODUCTION

STT-RAM is an emerging nonvolatile memory that has all the characteristics of a universal memory. It is nonvolatile, highly scalable, has low power consumption, unlimited endurance, high density and multilevel cell capability. In this paper preliminary investigations of switching speed and current capabilities of the basic STT-RAM memory cells for two different models i.e. In-plane and perpendicular magnetic anisotropy (PMA) has been done. The cell design is done using cadence tools in 45nm hybrid CMOS/MTJ process. The results show that the performance of STT-RAM cells is comparable to that of theoretical results.

2. STT-RAM TECHNOLOGY

The development of spintronics was due to the discovery of giant magnetoresistance (GMR) by [1, 2]. The main principle in spintronics is the manipulation of spin-polarized currents in contrast to traditional electronics where spin is ignored. As first suggested by Mott [3] spin-polarized currents can be generated by exploiting the influence of the spin on the transport properties of the electrons in ferromagnetic conductors. The discovery of tunneling magnetoresistance (TMR) followed the GMR. The important milestone was reached when S. Yuasa et al.[4] and Parkin et al. [5] showed that very large TMR ratios up to 200% at room temperature could be obtained with MgO Magnetic Tunnel Junction (MTJ).

The main element of the STT-RAM is the MTJ cell. The MTJ consists of two ferromagnetic layers separated by a barrier layer made of MgO as shown in figure 1. The MTJ resistance is determined by the relative magnetization directions of the two ferromagnetic layers. When the magnetization directions of the layers are parallel, the MTJ is in low resistance state (representing a bit 0), whereas if the layers are antiparallel, the MTJ is said to be in high resistance state (representing a bit 1). Data storage is realized by switching the MTJ between high and low resistance states. [7]
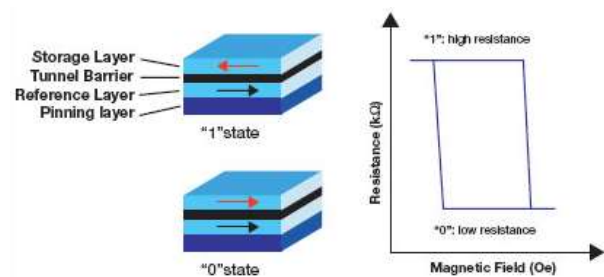

Figure 1. MTJ structure representing antiparallel ('1' state) and parallel ('0' state) [Alexander Driskill et al, Grandis corporation]

3. BASIC STRUCTURE OF STT-RAM MEMORY CELL

The basic structure uses an MTJ as the storage element and a N-channel MOSFET (1T-1MTJ) as the selection device.[8] Figure 2 shows the diagrams of the circuit and cross section of the structure. In the STT-RAM cell the source of the NMOS transistor is connected to the source line (SL). The free layer of the MTJ is connected to the bit line (BL) while the other pinned layer to the drain of NMOS. The word line (WL) is connected to the gate. In this arrangement the STT-RAM uses existing CMOS technology with additional 2-3 masks only.
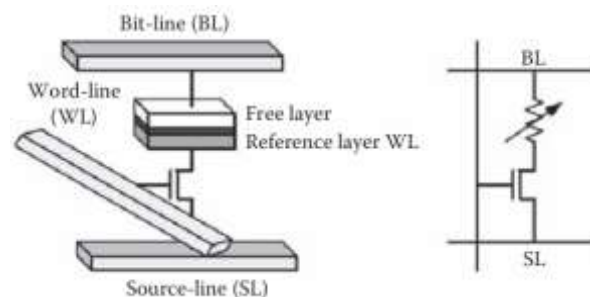

Figure 2. 1T-1MTJ STT-RAM (a) cross section and (b) circuit diagram

3.1 Read and Write Mechanisms

The switching of the states in MTJ is obtained by changing the direction of current through it. When writing '0' the current flows from BL to SL, whereas when writing '1' the current flows in opposite direction i.e from SL to BL. when the MTJ terminal is biased to VDD, the cell access transistor operates in the linear region and does not limit the current through the MTJ. Therefore a resistor is connected to limit the current through it. In the reverse bias case, the access transistor operates in a diode connected manner and thus the threshold drop across the access device limits the voltage drop across the MTJ. This voltage drop places an upper limit on the switching current that can be applied to the cell.

The data read operation is slightly different from that of conventional memory cell. The STT-RAM requires a reference voltage to compare the output generated by the sense amplifier. Generally the reference voltage is chosen as the voltage drop across the resistance $(R_L + R_H) / 2$ where R_L and R_H are the resistances of MTJ in parallel and anti-parallel states respectively. The read operation consists of making the word line as high, this selects the access transistor. By applying a read voltage to the selected memory cell, the generated current on the bit line can now be compared to the reference signal in the sense amplifier.

4. STT-RAM TECHNOLOGIES

There are two types of switching mechanisms in STT-RAM currently, the In-plane switching (IPS) and the perpendicular magnetic anisotropy (PMA) type. The PMA are advantageous over IPS anisotropy type for reducing switching current density in MTJ's. Devices with IPS magnetic anisotropy materials have to overcome additional demagnetizing fields. So STT-RAM devices with PMA are attracting much interest for STT-RAM applications. Perpendicular MTJ's with Tunnel magneto resistance (TMR) ratios up to 64% at room temperature are reported using rare earth transition metal alloys [9][10].

5. STT-RAM CELL DESIGNS

In addition to the one transistor-one MTJ (1T-1MTJ) structure shown in Figure 2 several other cell designs like two transistor-one-MTJ (2T-1MTJ) [11] and thermally assisted MRAM (TAS-RAM) also exist. [12] The 1T-1MTJ cell has the advantage of less area but it is vulnerable to process variations and thus cell stability is less. J. Li et al [11] proposed the 2T-1MTJ cell model which is more robust to process variations. This model compensates cell instability during read operations and improves write operation by sacrificing the area. Therefore memory density is less compared to 1T-1MTJ cell.
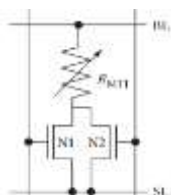

Figure 3. 2T-1MTJ STT-RAM cell

The 2T-1MTJ cell consists of two NMOS transistors, one for read (N1) and the other for write operation (N2) as shown in figure 3. During the read operation only the read NMOS is turned on whereas during write operation both the read and write NMOS are turned on to provide large current for better

write stability. This technique provides more robustness than the 1T-1MTJ cell. However the cell area increases due to the two transistors.

6. SIMULATION RESULTS

In our work we have used the two types of STT-RAM models i.e IPS and PMA type and designed the basic memory cells as mentioned in the previous section. The design has been carried out in 45nm technology using cadence tools and simulation results have been obtained. The results are as follows: Figure 4 (a) shows the schematic of IPS 1T-1MTJ cell and Figure 4(b) its simulation outputs. Figure 5(a) and 5(b) shows the 1T-1MTJ results obtained using PMA model.
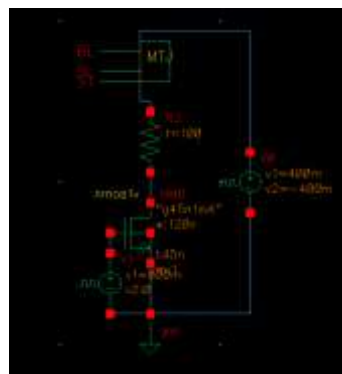

Figure 4(a) : Schematic of 1T-1MTJ cell (IPS)

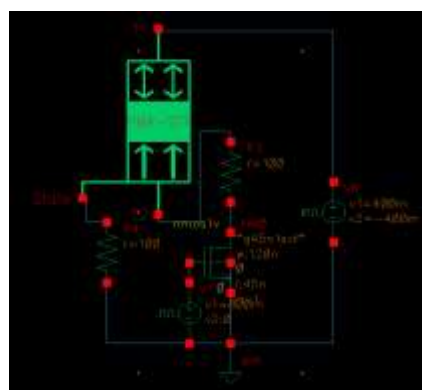Figure 4(b) : Outputs of 1T-1MTJ cell (IPS)

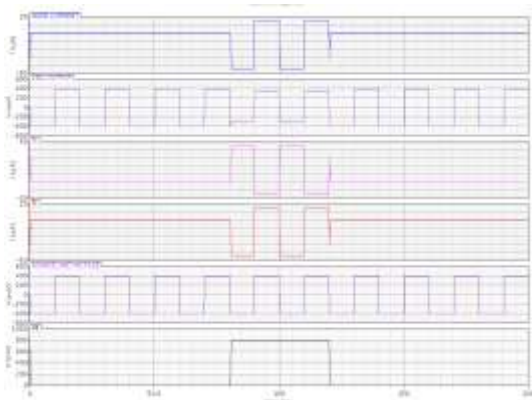Figure 5(a) : Schematic of 1T-1MTJ cell (PMA)

Figure 5(b) : Outputs of 1T-1MTJ cell (PMA)

Similarly, Figure 6(a) and (b) respectively shows the schematic and simulation outputs of 2T-1MTJ IPS type and finally Figure 7(a) and (b) the schematic and outputs of 2T-1MTJ for PMA model.
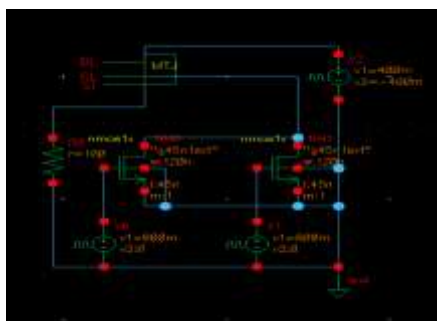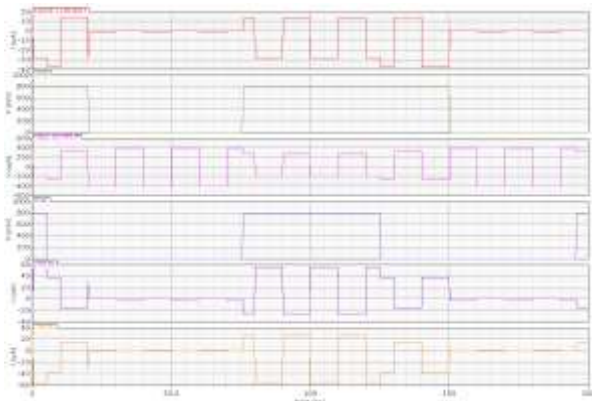

Figure 6(a) : Schematic of 2T-1MTJ cell (IPS)

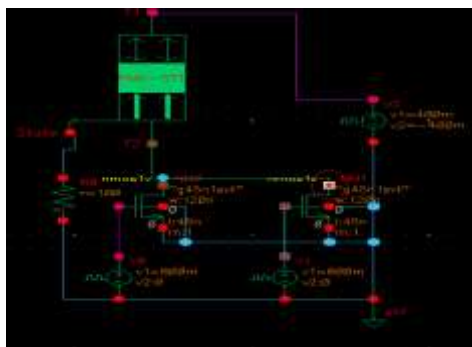Figure 6(b) : Outputs of 2T-1MTJ cell (IPS)

Figure 7(a) : Schematic of 2T-1MTJ cell (PMA)

Figure 7(b) : Outputs of 2T-1MTJ cell (PMA)

7. CONCLUSIONS

In this paper, design of basic STT-RAM memory cells has been carried out in 45nm technology node. Two types of models have been used, the IPS and the PMA type. Using these models we have designed two types of memory cells i.e the 1T-1MTJ and 2T-1MTJ type. The results show that the write current for IPS 1T-1MTJ is approx. 35µA and for PMA type it is around 30 µA. Similarly the write current for 2T-1MTJ of PMA type is approx. 50 µA compared to 55 µA drawn by IPS type.

The results clearly show that the write current for PMA type is less when compared to IPS type for both the memory cells. However, the switching speed of both types are nearly the same.

8. ACKNOWLEDGMENTS

9. REFERENCES

[1] M.N. Baibich, J.M. Broto, A. Fert et al, Giant magneto-resistance of (001)Fe/(001) Cr magnetic superlattices, Phys. Rev. Lett. 61, 2472–2475(1988)

[2] G. Binash, P. Grünberg, F. Saurenbach et al , Enhanced magnetoresistance in layered magnetic structures with antiferromagnetic interlayer exchange, Phys. Rev. B 39, 4828–4830 (1989).

[3] N. F. Mott, The electrical conductivity of transition metals, Proc. Roy. Soc. A 153, 699–718 (1936).

[4] S. Yuasa, T. Nagahama,K. Fukushima et al, Giant room-temperature magnetoresistance in single-crystal Fe/MgO/ Fe magnetic tunnel junctions, Nat. Mater. 3, 868–871 (2004)

[5] S.S.P Parkin, C. Kaiser, A. Panchula et al , Giant tunneling magnetoresistance at room temperature with MgO (100) tunnel barriers, Nat. Mater. 3, 862–867 (2004)

[6] 236601Xu,W , Sun, H., Wang, X. Chen, Y., and Zhang, T (2009) Design of last‑level on‑chip cache using spin‑torque transfer RAM (STT-RAM). IEEE Transactions on Very Large Scale Integration Systems, 19:1–11

[7] Zhang, S. Levy, P. M, and Fert, A. (2002) Mechanisms of spin‑polarized current driven magnetization

switching, Physical Review Letters, 88: Very Large Scale Integration Systems, 19: 1–11.

[8] Prejbeanu, I. L, Kerekes, M, Sousa, R.C. Sibuet, H. Redon, O. Dieny, and Nozières, J. P. (2007). Thermally assisted MRAM Journal of Physics: Condensed Matter, 19:165218.

[9] M. Nakayama, T. Kai, N. Shimomura, M. Amano, E. Kitagawa, T. Nagase,M. Yoshikawa, T. Kishi, S. Ikegawa, and H. Yoda, J. Appl. Phys.103, 07A710 (2008).

[10] H. Ohmori, T. Hatori, and S. Nakagawa, J. Appl. Phys. 103, 07A911 (2008).

[11] Li. J. Liu, H. Salahuddin, S. and Roy, K. (2008) Variation tolerant spin torque transfer (STT) MRAM array for yield enhancement Paper presented at the IEEE Custom Integrated Circuits Conference (CICC) San José, CA.

[12] Deac, A. Redon, O. Sousa, R. C. Dieny, B. Nozières, J. P. Zhang, Z. Liu Y, and Freitas, (2004) Current driven resistance change in low resistance x area magnetic tunnel junctions with ultra‑thin Al‑Ox barriers. Journal of Applied Physics, 92: 6792 – 6794.